Ultrastrong Freestanding Graphene Oxide Nanomembranes with Surface Enhanced Raman Scattering Functionality by Solvent Assisted Single-Component Layer by Layer Assembly

Rui Xiong,[†,‡,#] Kesong Hu,[‡,#] Shuaidi Zhang,[‡] Canhui Lu,[†] and Vladimir V. Tsukruk*[,‡]

[†]State Key Laboratory of Polymer Materials Engineering, Polymer Research Institute of Sichuan University, Chengdu 610065, China.

[‡]School of Materials Science and Engineering, Georgia Institute of Technology, Atlanta, GA 30332-0245, USA

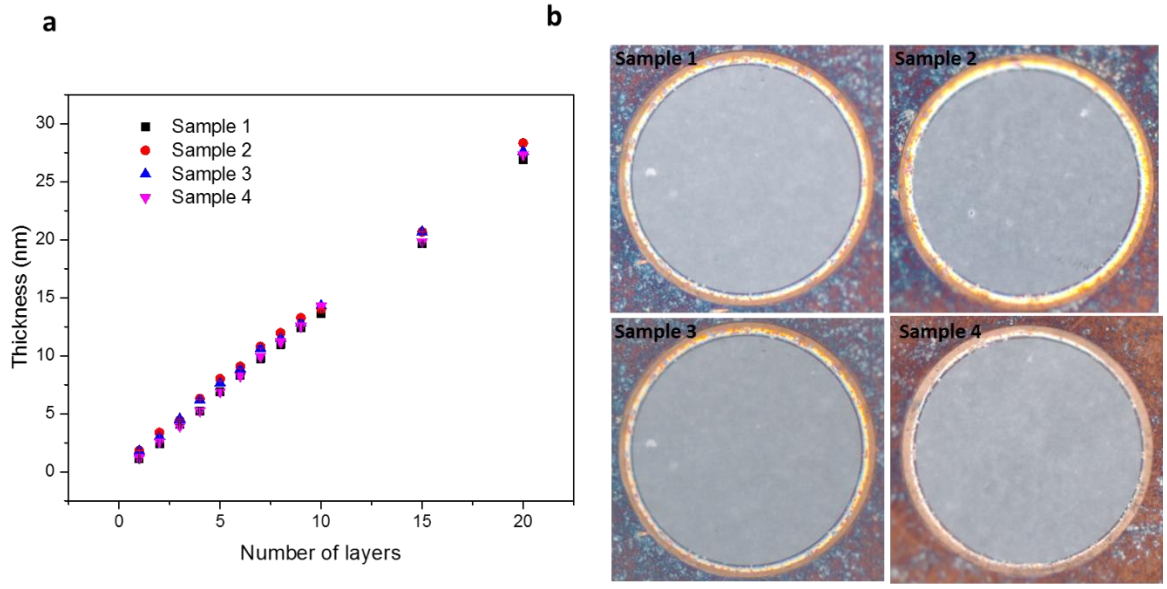

Figure S1 (a)The thickness growth of different GO nanomembranes samples with the increase of deposited layers; (b) rGO nanomembranes from different samples suspended on copper grid with 300 μm aperture.

Figure S2a and b show the typical freestanding polystyrene (PS) nanomembrane and cellulose acetate (CA) nanomembrane overlayed by PS layer. The CA/PS nanomembranes show lightly red structure color, which induced by the different reflective index of CA and PS. For the hydrophobic nanomembranes, such as PS, can be released from the silicon wafer substrate directly with any supporting layer due to the strong surface tension of nanomembranes and silicon water (Figure S2c). However, for the hydrophilic nanomembranes, such as CA, the surface tension is not strong enough to overcome the interaction of nanomembrane and substrate. Therefore, the hydrophobic overlay layer is necessary to enhance the surface tension and the overlay layer can be easily removed after transferred onto the target substrate.

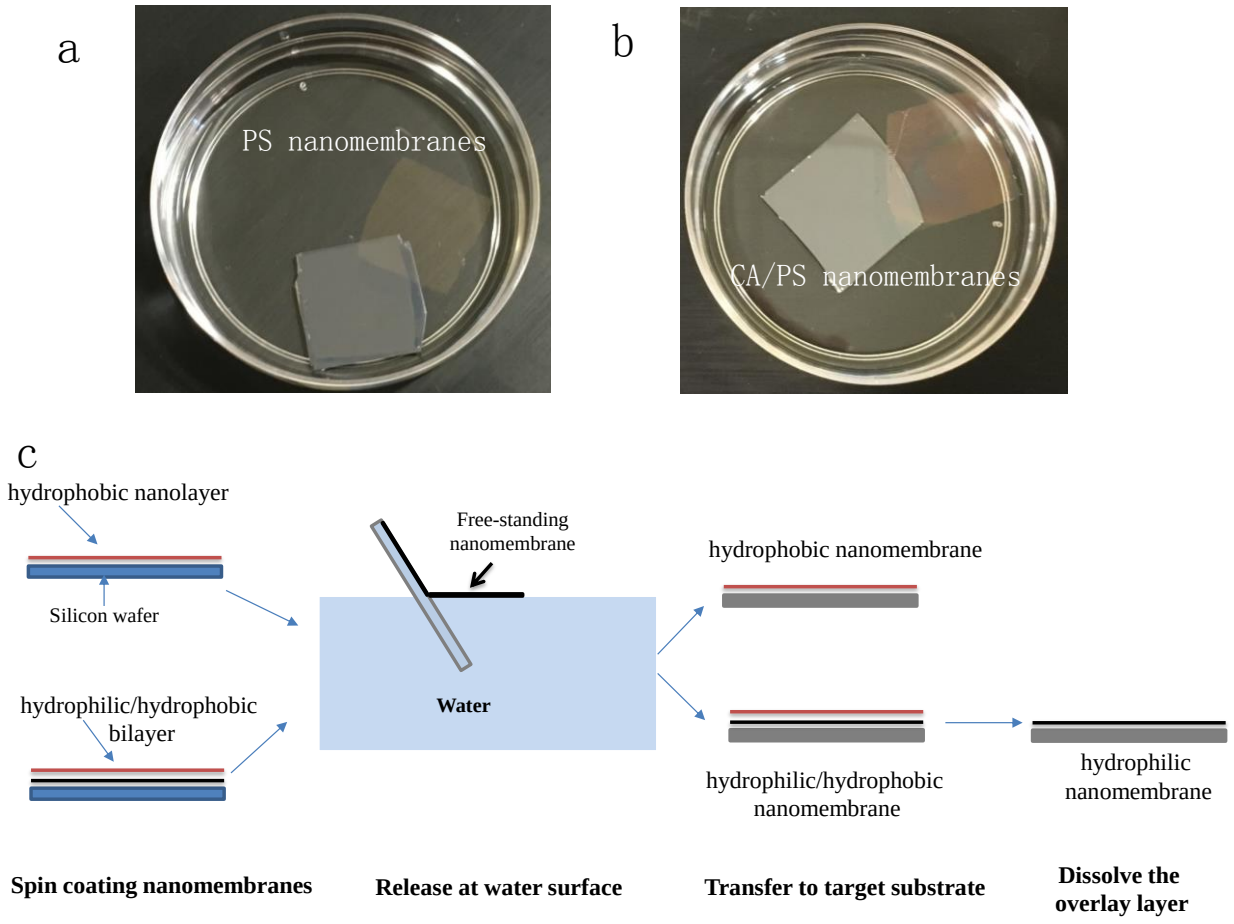

Figure S2 The freestanding (a) PS nanomembrane and (b) CA/PS bilayer nanomembrane. (c) The schematic illustration of the preparation of other free-standing hydrophobic and hydrophilic nanomembranes.

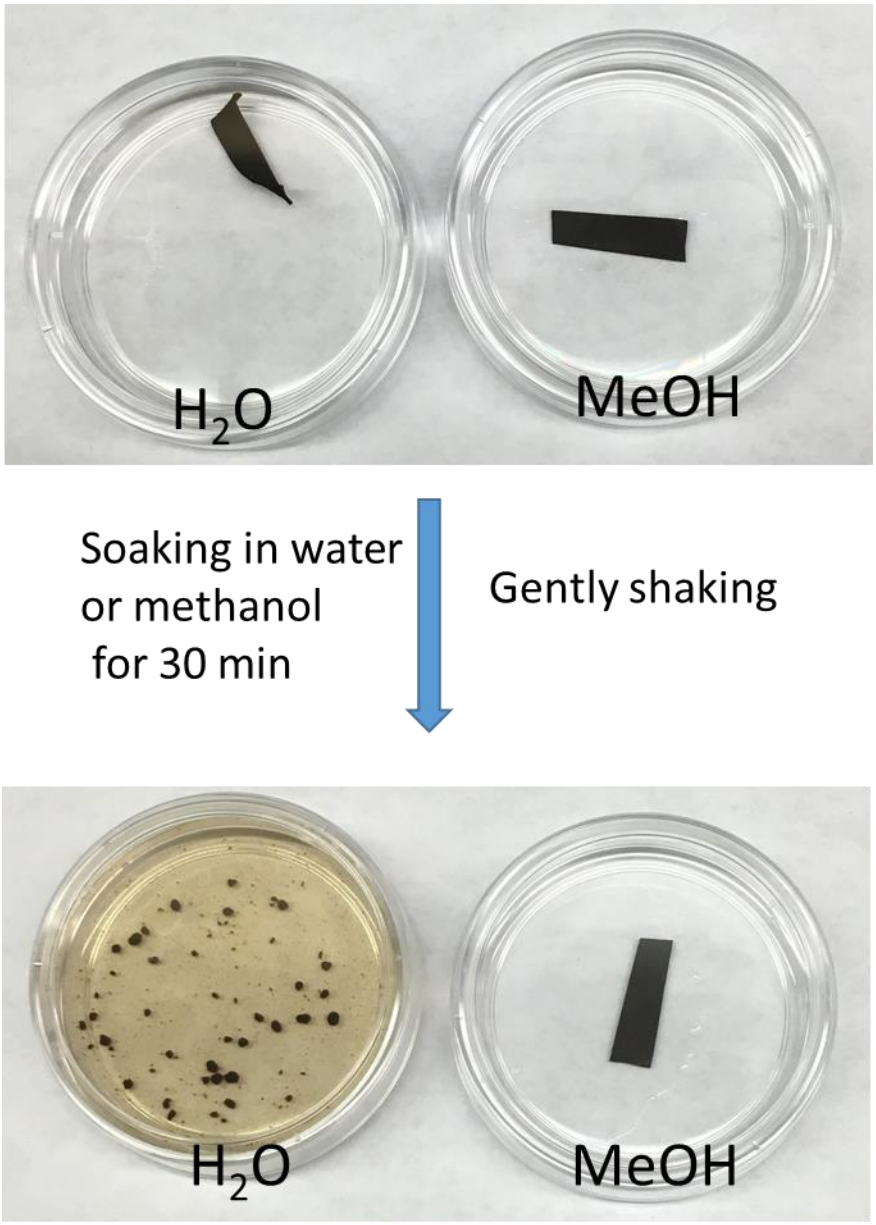

Figure S3 Dissolving test of water and methanol to graphene oxide paper by VAF technique.

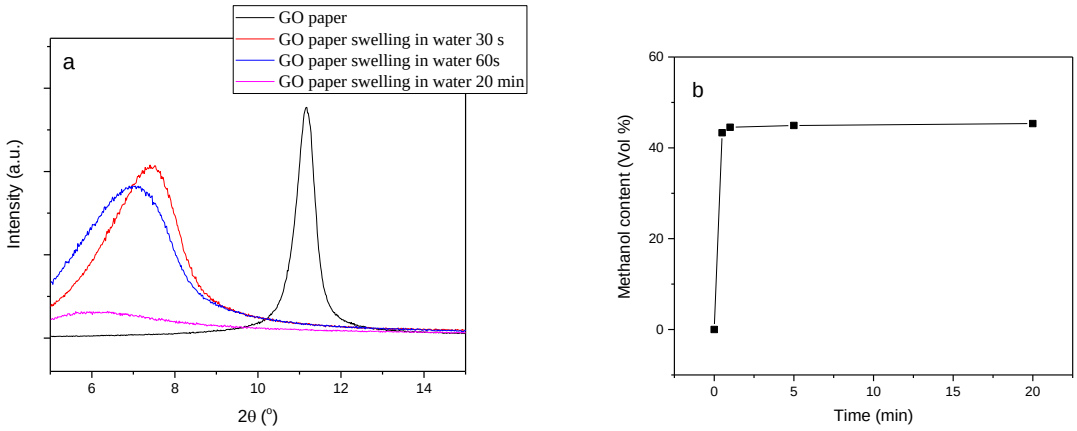

Figure S4 X-ray Diffraction of GO paper in the water disolving test; (a) the XRD curves and (b) methanol content of GO swelling in methanol for different time.

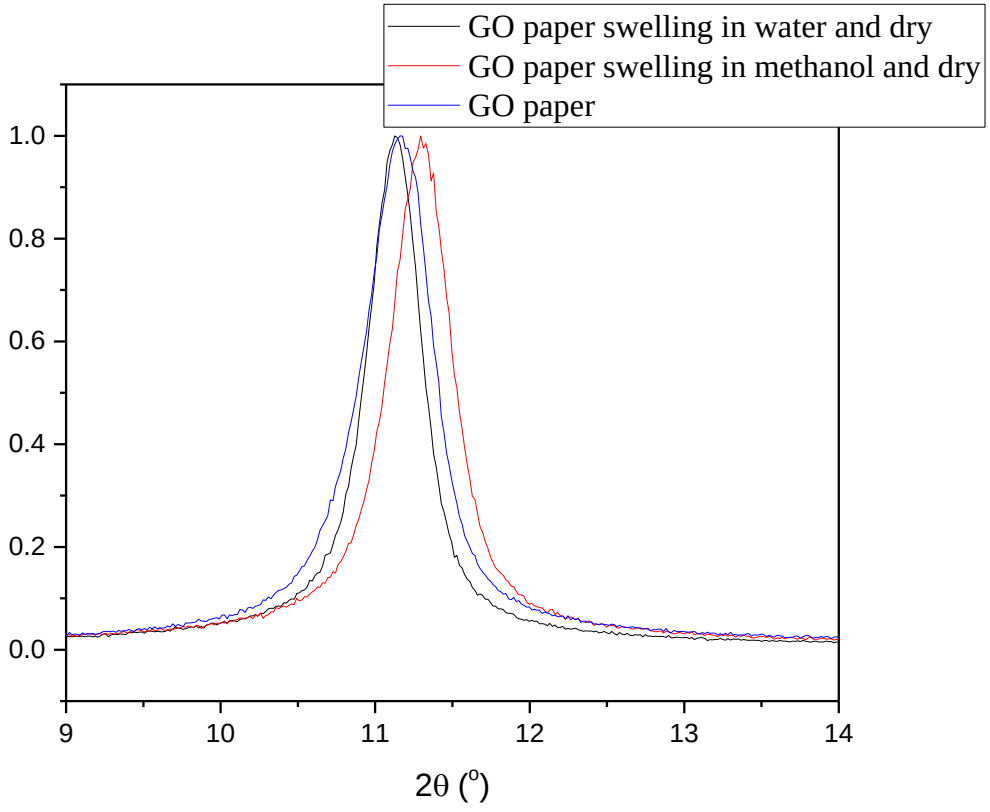

Figure S5 The X-ray Diffraction of GO paper totally dried after the swelling in water and methanol.

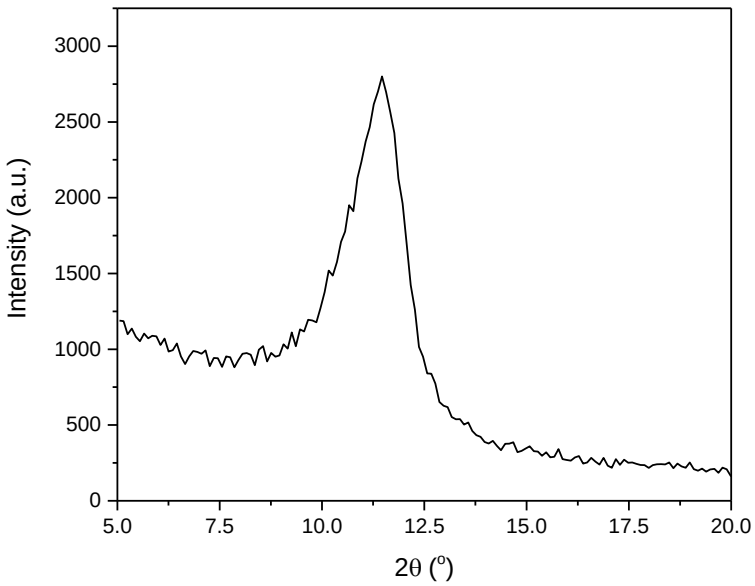

Figure S6 X-ray Diffraction of LbL GO nanomembranes prepared from methanol solution.

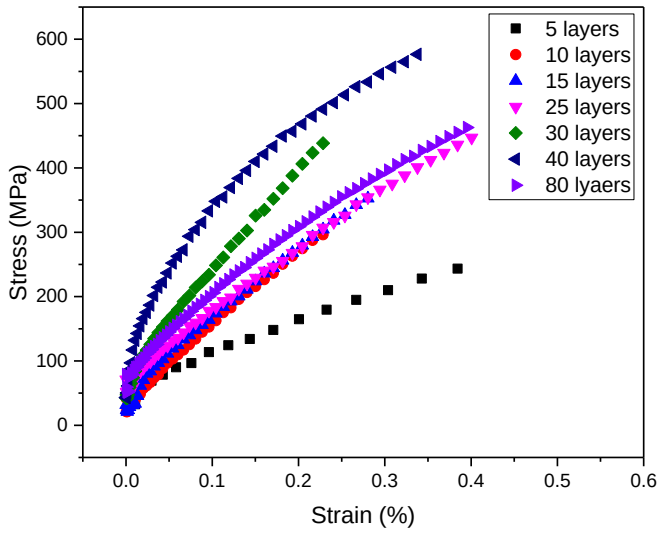

Figure S7 The typical stress-strain curves of LbL rGO nanomembranes with different layers fabricated from methanol solution.

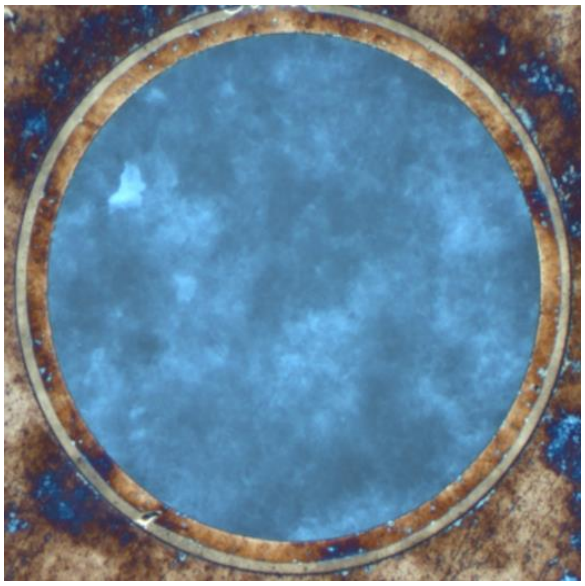

Figure S8 The optical microscope image of 10-layer LbL rGO nanomembranes on copper grid with 300 µm aperture.

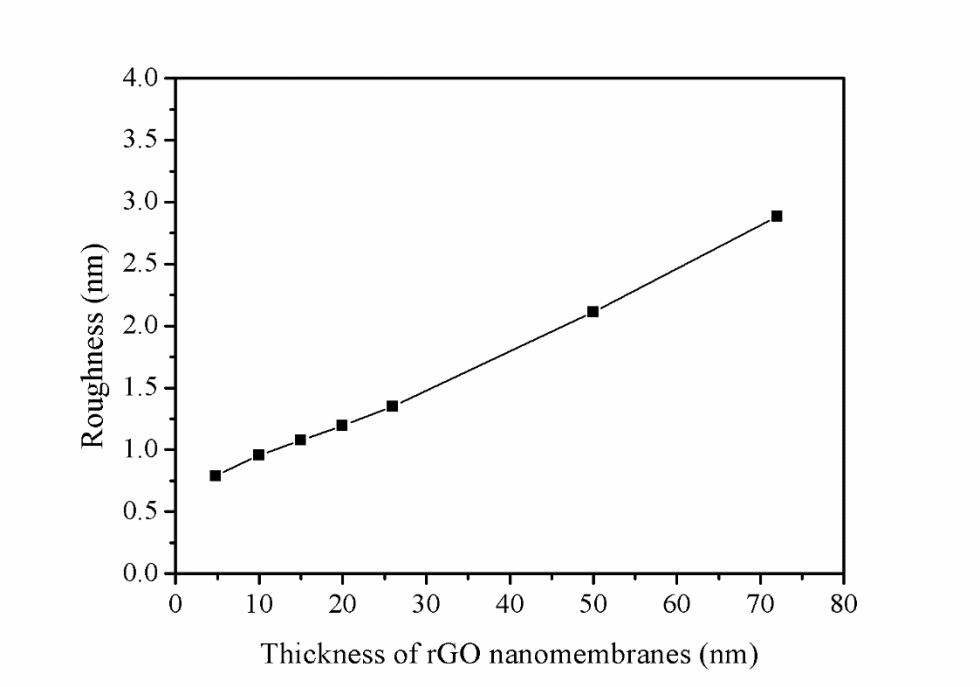

Figure S9 The roughness (5×5 µm) of rGO nanomembranes with various thickness.

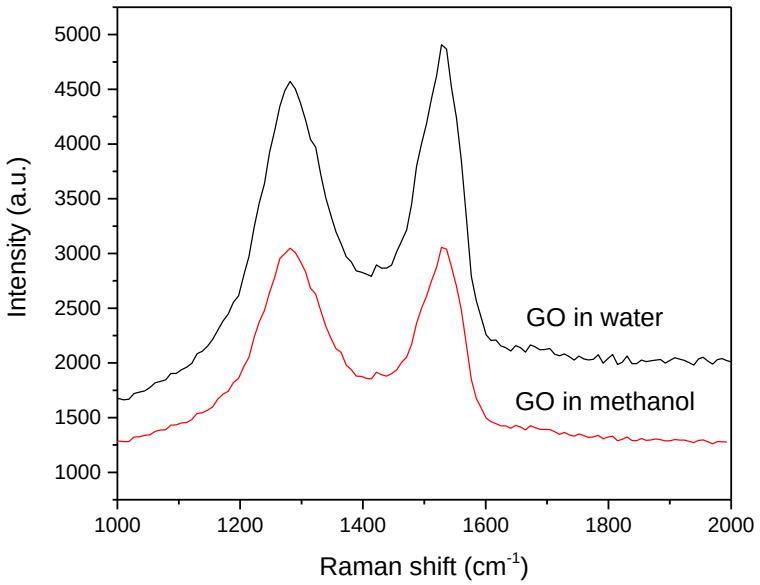

Figure S10 The Raman spectrum of GO nanomembranes prepared from water and methanol by drop cast.

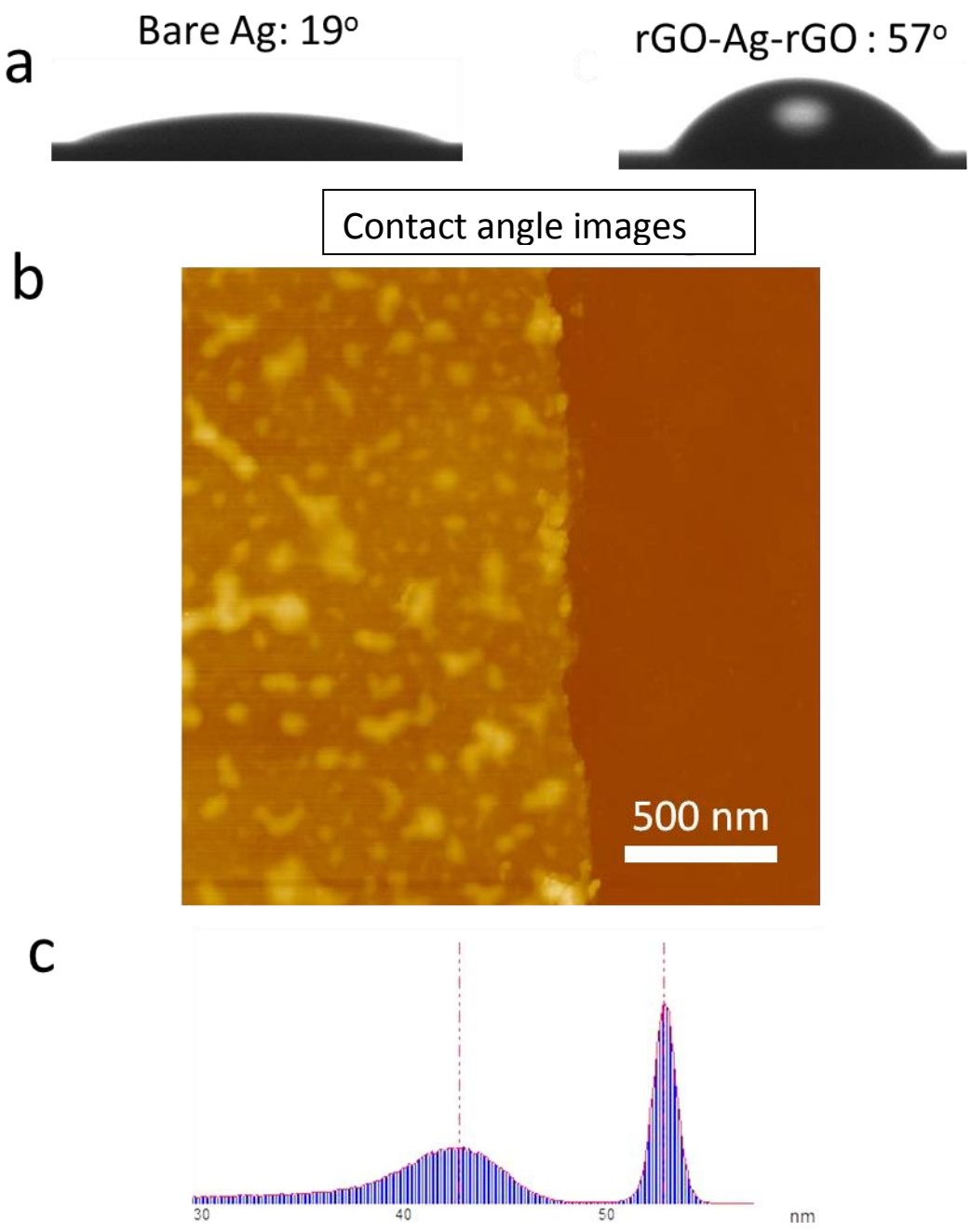

Figure S11 (a) Water contact angel of bare Ag nanoplates and Ag nanoplates encapsulated into the rGO nanomembrane; b) AFM images of nanomembrane edge; Z scale = 100 nm. c) Bearing analysis of this AFM image to determine the average nanomembrane thickness.

To prove the SERS spectra obtained from rGO/Ag/rGO is more reproducible than pure Ag NPs, we recorded the Raman spectra from 12 different spots. As shown in the Figure S12, the background of rGO/Ag/rGO is much better than the that of bare Ag due to the quenching of dye fluorescence by the rGO. Besides, the signal variation of rGO/Ag/rGO is obviously smaller than pure Ag, resulting from the isolation of target molecule and SERS substrate. We also zoomed in the peaks at 620 cm^{-1} marked by the red ovals, the deviation of rGO/Ag/rGO is much smaller than Ag NPs (variation: 4.4% vs 21.4%). Additionally, the SERS spectra obtained from Ag NPs shows a lot of additional peaks (marked by the red arrows), resulting from the secondary and mixed vibrational modes and potentially locally damaged R6G molecules. We have to mention that the reproducibility of rGO/Ag/rGO demonstrated here is modest, when compared with monodispersed metallic nanoparticles. This is because the SERS enhancement in this case is generated by the rough surface of the micron-sized Ag nanoplates, which have much worse uniformity than monodispersed metallic nanoparticles (such as metallic nanocubes and nanorods).

The rGO/Ag/rGO shows slightly lower SERS intensity than bare Ag NPs, which is inevitable for these ultrathin coating even for these 1 atom thick graphene coating.[1] However, the SERS spectrum obtained from rGO/Ag/rGO shows cleaner background than Ag NPs due to quenching of dye fluorescence, which, under certain circumstances, might be strong enough to entirely mask the Raman peaks and cannot be corrected through data smoothing. Even it is possible to be fixed by plot smoothing/baseline correction in some case, there is no doubt that these post-processing will increase the unnecessary cost.

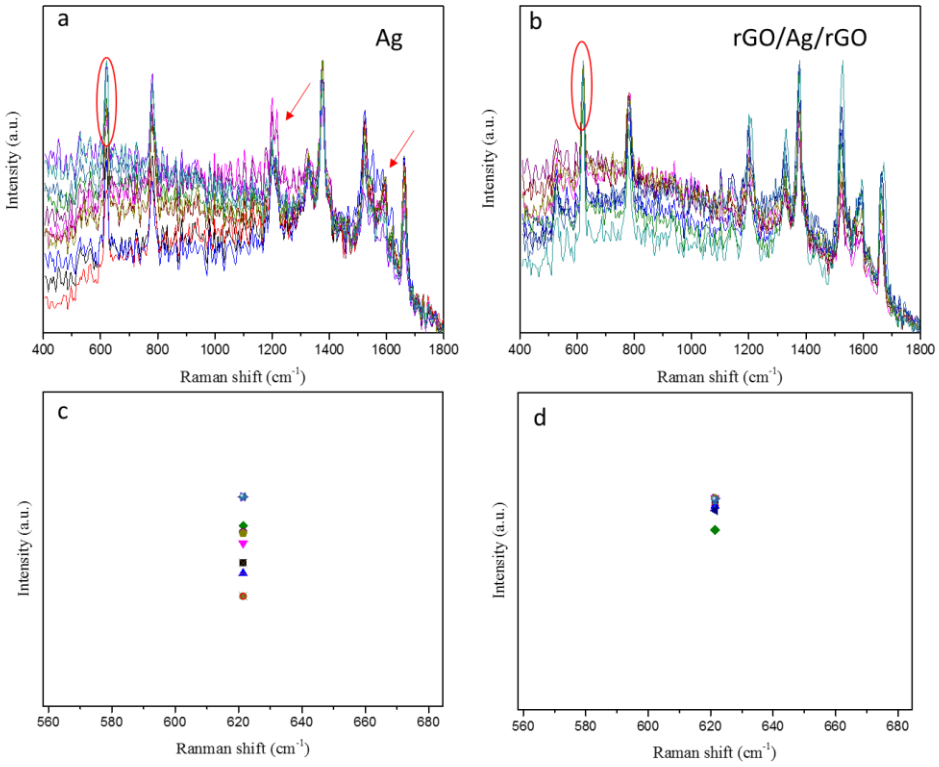

Figure S12 The SERS spectrum of Ag (a) and rGO/Ag/rGO (b) obtained from 12 different sports. The variation of peak intensity of Ag (c) and rGO/Ag/rGO (d) at 620 cm^{-1} marked by red oval.

These freestanding rGO-Ag-rGO SERS were ultrathin, mechanically robust and flexible, and optically transparent, which can be easily transferred and conformally coated on various topologically complex surfaces (paper and Al foil, and glass) as shown in the following Figure S13. These as-prepared soft rGO-Ag-rGO nanomembranes can be served as a unique sensing platform for chemical identification, compared with these intractable pure nanoparticles dispersion.[2]

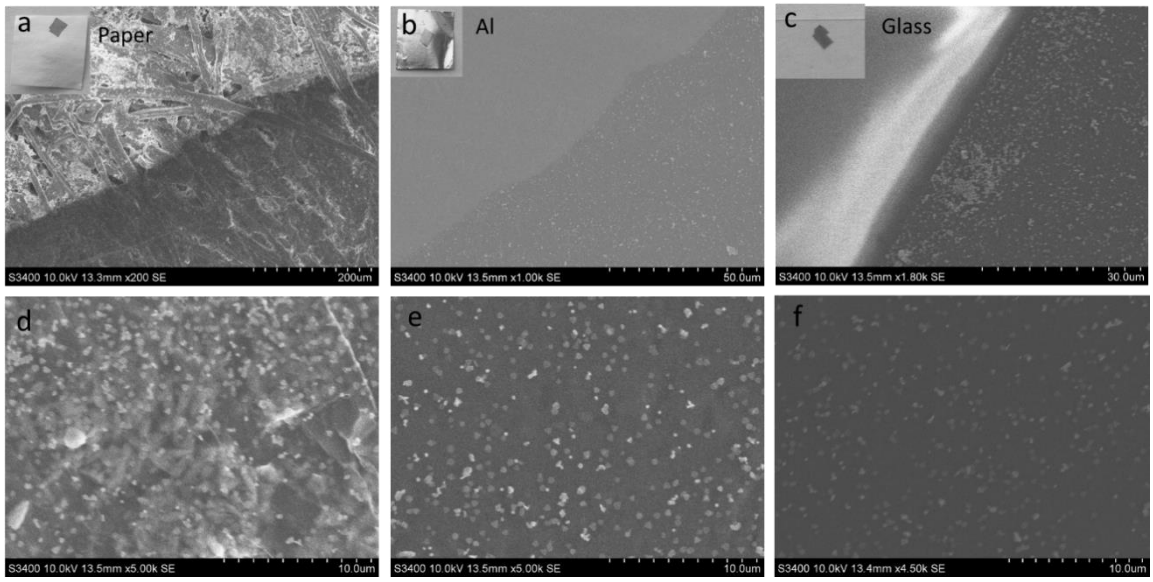

Figure S13 The freestanding rGO-Ag-rGO SERS coated on paper (a and d), Aluminium foil (b and e) and glass (c and f)

The wet stability of SERS substrate is a very important in the actual application, as in many case these SERS substrates have to be exposed to liquid environment to detect chemicals of interest. Notably, these freestanding rGO-Ag-rGO nanomembranes show much better wet stability than pure Ag NPs due to the shielding effect of ultrastrong rGO nanomembranes. The Figure S14 shows the Ag NPs (a and b) and rGO-Ag-rGO (c and d) on silicon wafer before and after ultrasonic treatment in water for 30 min. Obviously, most of the Ag NPs for bare Ag substrate were detached from the silicon substrate after ultrasonic treatment due to the weak interaction between Ag NPs and the substrate, while rGO-Ag-rGO retained its original nanostructure. This is because rGO is highly impermeable to all gases, liquids and aggressive chemicals. The exceptional barrier properties are attributed to highly dense and almost defect-free layered nanostructure.[3]

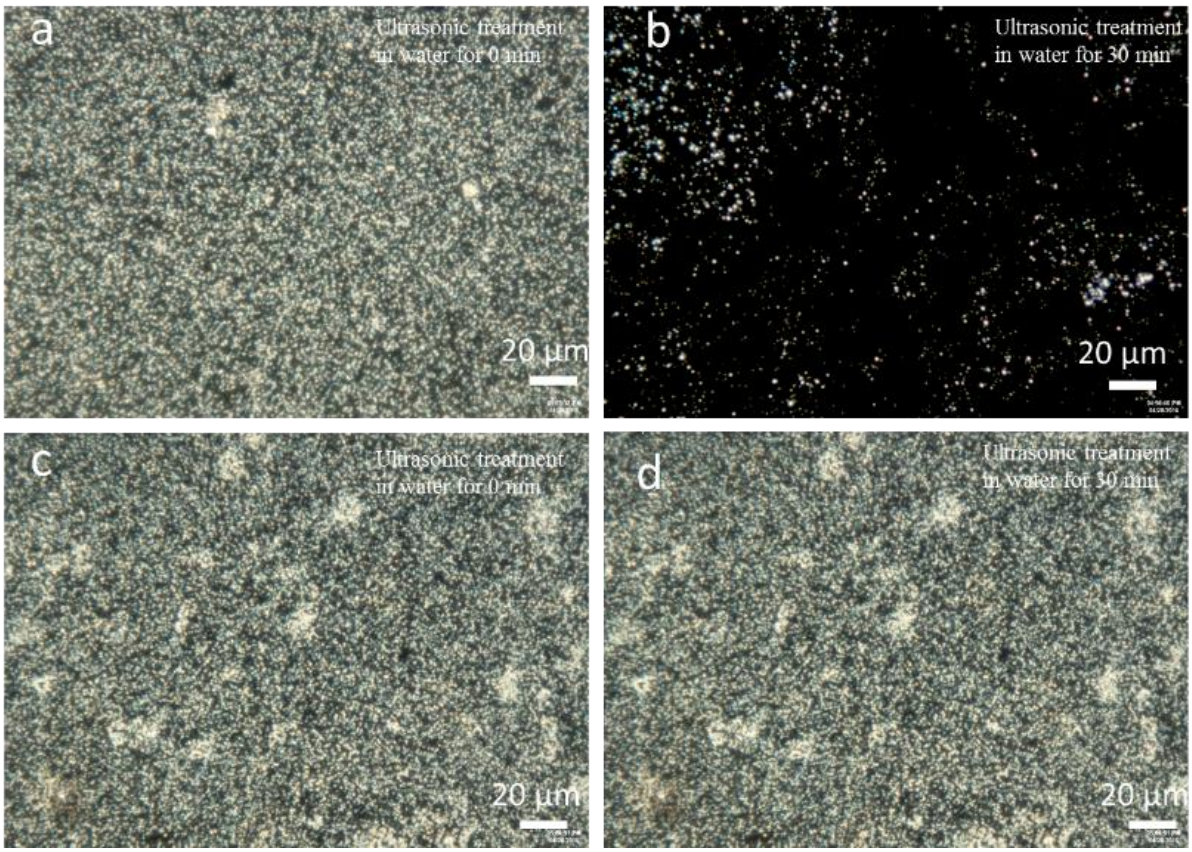

Figure S14 Wet stability of bare Ag NPs (a and b) and rGO/Ag/rGO (c and d) before and after ultrasonic treatment in water for 30 min.

For Ag nanoparticle based SERS substrate, an important property we are concerned with is the anti-oxidation, because Ag nanoparticles without any protective coating is very easy to be oxidized. However, in our nanomembranes, these silver NPs demonstrate better anti-oxidation than pure Ag NPs due to highly impermeable rGO as protective layer. The Figure S15 shows the XPS Ag-3d spectrum of Ag and rGO/Ag/rGO after treated in air at 200 °C for 2 h. A right-shifted Ag^0 peak at 368.6 eV can be obviously observed for Ag, compared with the peak of rGO/Ag/rGO at 368.8 eV, indicating that the Ag NPs contains a small amount of Ag_2O content. This protective coating of rGO on metal surface to enhance the anti-oxidation has been widely reported in the previous studies.[4,5]

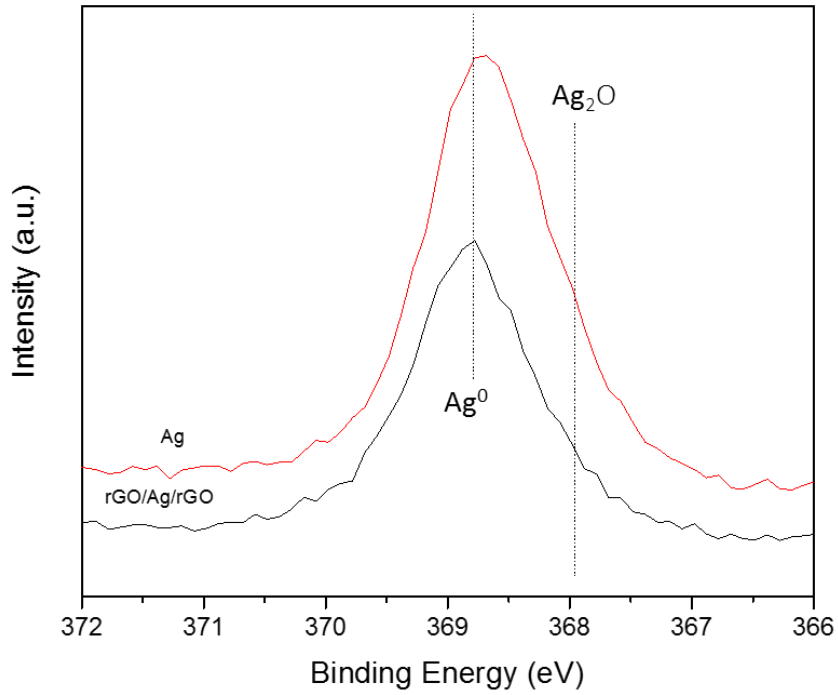

Figure S15 The XPS Ag-3d spectrum of Ag and rGO/Ag/rGO after thermal treated at 200 ^{o}C for 2 h.

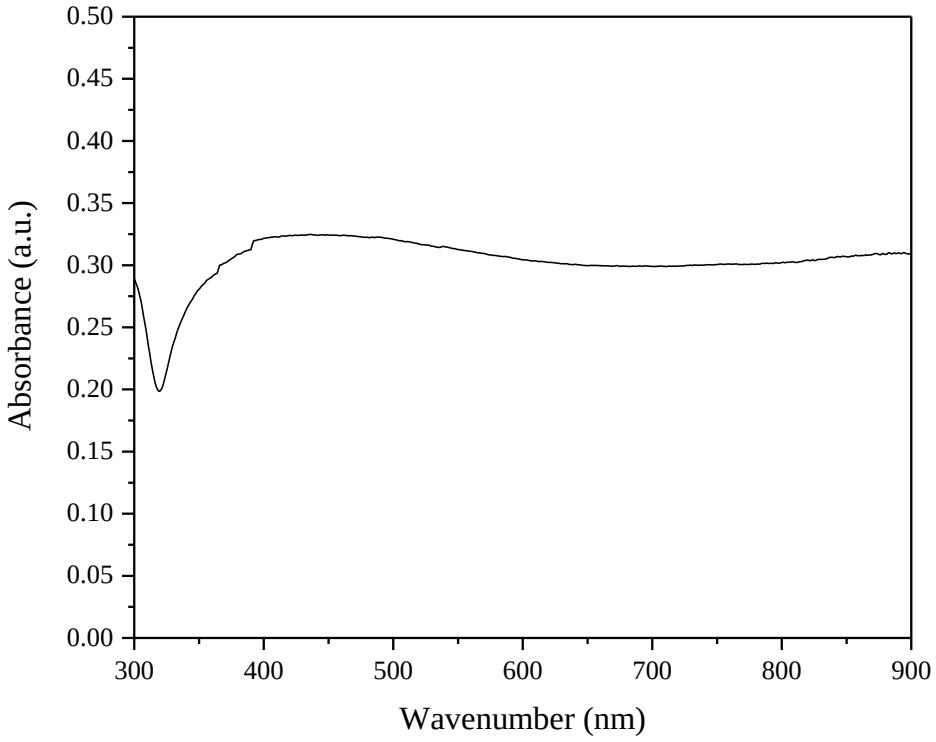

Figure S16 The UV-VIS absorption spectra of Ag nanoplates.

Reference

1. Xu, W.; Ling, X.; Xiao, J.; Dresselhaus, M. S.; Kong, J.; Xu, H.; Liu, Z.; Zhang, J. Surface Enhanced Raman Spectroscopy on a Flat Graphene Surface. *Proc. Natl. Acad. Sci*. **2012**, *109*, 9281-9286.
2. Chen, Y.; Si, K. J.; Sikdar, D.; Tang, Y.; Premaratne, M.; Cheng, W. Ultrathin Plasmene Nanosheets as Soft and Surface-Attachable SERS Substrates with High Signal Uniformity. *Adv. Optical Mater.* **2015**, *3*, 919-924.
3. Su, Y.; Kravets, V. G.; Wong, S. L.; Waters, J.; Geim, A. K.; Nair, R. R. Impermeable Barrier Films and Protective Coatings Based on Reduced Graphene Oxide. *Nat. Commun.* **2014**, *5*.
4. Kang, D.; Kwon, J. Y.; Cho, H.; Sim, J.-H.; Hwang, H. S.; Kim, C. S.; Kim, Y. J.; Ruoff, R. S.; Shin, H. S. Oxidation Resistance of Iron and Copper Foils Coated with Reduced Graphene Oxide Multilayers. *ACS Nano* **2012**, *6*, 7763-7769.
5. Chen, S.; Brown, L.; Levendorf, M.; Cai, W.; Ju, S.-Y.; Edgeworth, J.; Li, X.; Magnuson, C. W.; Velamakanni, A.; Piner, R. D.; Kang, J.; Park, J.; Ruoff, R. S. Oxidation Resistance of Graphene-Coated Cu and Cu/Ni Alloy. *ACS Nano* **2011**, *5*, 1321-1327.